

Supporting information for

**Oxygen, Nitrogen Co-doped Molybdenum Disulphide Nanoflowers for
Excellent Antifungal Activity**

Parbati Basu¹, Khushi Mukherjee², Sudipta Khamrui³, Subharaj Mukherjee⁴, Maudud Ahmed⁴, Krishnendu Acharya², Debmalya Banerjee³, Padinharu M.G. Nambissan⁴, and Kuntal Chatterjee*¹

¹Department of Physics, Vidyasagar University, Midnapore-721102, India

²Molecular And Applied Mycology And Plant Pathology Laboratory, Department of Botany, University of Calcutta, Kolkata-700019, India

³Department of Physics, IIT Kharagpur, Kharagpur-721302, India

⁴Applied Nuclear Physics Division, Saha Institute of Nuclear Physics, Bidhannagar, Kolkata-700064, India

**Corresponding Author: Email: kuntal@mail.vidyasagar.ac.in*

Table of Contents:

S1.1 Positron Annihilation Spectroscopy Studies	S3
S1.2 Fungitoxicity Assay	
S1.2.1 Growth inhibition Test	S4
S1.2.2 TTC Assay	S4
S1.2.3 Microscopic Analysis	S4
S1.2.4 Fluorescence Microscopy Studies	S5
Figure S1 N ₂ adsorption desorption isotherm for ONMS and NMS	S6
Figure S2 Splitting of E_{2g} Raman mode for ONMS and NMS due to doping.....	S6
Figure S3 High resolution XPS spectrum from O 1s for ONMS and NMS.....	S7
Figure S4 Survey spectrum analysis for ONMS and NMS	S7
Figure S5 Digital plate photographs of colony formation units for ONMS.....	S8
Figure S6 Digital plate photographs of colony formation units for NMS	S9
Figure S7 Digital plate photographs of colony formation units for MS.....	S10
Figure S8 Dose dependent fungitoxicity assessment of ONMS by TTC assay	S11
Table S1 Summary of Antifungal studies of 2D layer based fungicides	S12
S1.3 Biocompatibility assay of ONMS	
S1.3.1 Experimental	S12
S1.3.2 Results	S13
S1.3.3 Discussion	S13
Figure S9 Biocompatibility assay of ONMS	S14
References	S15

S1.1 Positron Annihilation Spectroscopy Studies:

To perform the positron annihilation spectroscopy(PAS) experiments, a ^{22}Na ($\approx \mu\text{Ci}$) radioactive isotope was carefully inserted with precision at the geometrical centre of the bulk of the powdered samples taken in a glass tube having an approximate diameter of 10 mm. The powdered samples were taken in adequate amounts so that the ^{22}Na source is wholly embedded within it and no positron is able to penetrate to the walls of the glass container thereby ensuring that the annihilation of the positrons take place within the extent of occupancy of the sample. To prepare the source, $^{22}\text{NaCl}$ was deposited on a thin Ni foil ($\sim 2 \text{ mg/cm}^2$) which was annealed prior to the deposition of source in an adequately vacuumed atmosphere at 1050°C for 120 minutes. The protruding part of the Nickel foil was folded along a line remote to the source deposited area in order to cover the source. During acquisition of the experimental data, the glass tube in which the sample powders were taken was continuously evacuated to ensure complete removal of air or any other adsorbed gases on the sample. For positron lifetime measurements, BaF_2 scintillators along with XP2020Q photomultiplier tubes detected the emitted gamma rays. The positron annihilation lifetime measurements were performed using slow-fast gamma-gamma positron lifetime spectrometer equipped to have a time resolution(FWHM of ^{60}Co gamma rays coincidence spectrum) of 180 ps under the selected ^{22}Na experimental energy settings. Typically, under each spectrum almost 10^5 counts were recorded. The recorded data was analysed with the PALSfit program.¹

For the coincidence Doppler broadening spectroscopy(CDBS) measurements, two highly pure germanium detectors having an energy resolution of 1.27 keV and 1.33 keV were used to detect the gamma ray events E_1 and E_2 at the annihilation gamma ray energy of 511 keV. A two-parameter spectrum with $E_1 + E_2$ and $E_1 - E_2$ as the coplanar axes and counts distributed accordingly was generated from their time correlation. The ratio curves of the powdered samples studied was obtained by the projection of the segment under $E_1 + E_2 =$

1022 ± 2.4 eV onto the axis parallel to $E_1 - E_2$ followed by an analysis by the quotient method. The CDBS data acquisition, storage and analysis were all done making use of the LAMPS software designed and developed by the Pelletron division of TIFR, Mumbai.

S1.2 Fungitoxicity assay:

S1.2.1 Growth inhibition test:

Fungal mycelia (5mm diameter) from freshly grown colonies were inoculated into the nanoparticle (MS, NMS and ONMS) incorporated PDA plates and allowed to grow for 5-8 days at 30°C temperature. Radial growth of the developed fungal colonies was measured and compared with the control plate (devoid of NP). Experiments were performed under dark and visible light exposure. All experiments were conducted thrice for confirmation and triplicates were maintained for each set.

S1.2.2 TTC assay:

Fungal mycelia of 5mm diameter were incubated with different concentrations of MoS₂ nanosheets (ONMS) at 30 °C temperature. After 24 hours, 200 µl of TTC (Triphenyl Tetrazolium Chloride) reagent (5mg/ml) was incorporated to the fungal mycelia and nanoparticle suspensions and incubated for further 12 hours. The experiment was conducted under visible light illumination. The dehydrogenase enzyme, released by live fungal cells reduced TTC to triphenyl formazan (red colored), which was dissolved in dimethyl sulfoxide (DMSO) and detected by UV-visible spectroscopy at 570 nm.

S1.2.3 Microscopic analysis:

Scanning Electron Microscopy Analysis: Nanoparticle induced morphological deformities on fungal biomass were studied under scanning electron microscopy (SEM, ZEISS EVO 18 Special Edition) and compared with the untreated fungal biomass.

S1.2.4 Fluorescence Microscopy studies:

ONMS nanoflower induced ROS generation and its subsequent effect on fungal mycelia were also studied by fluorescence microscopy (Leica DM IL LED S-80; with Leica Application Suite V.4.7.1 software).

Nanoparticle induced reactive oxygen species (ROS) generation was studied by fluorescence microscopy using Dichlorofluorescein (DCF) dye. Briefly, fungal mycelia were grown in nanoparticle amended PD broth medium, followed by 24 h incubation at 30 °C. Next, DCF (3 μ M) was added into the broth medium and ROS production was determined using fluorescence microscope upon blue excitation.

In order to determine fungal cell death, MoS₂ treated fungal mycelia were mixed with EtBr (Ethidium bromide) and observed under fluorescence microscope upon green excitation. In, non-viable fungal biomass, EtBr entered through the perforated cell wall and binds to the DNA material and emits red fluorescence.

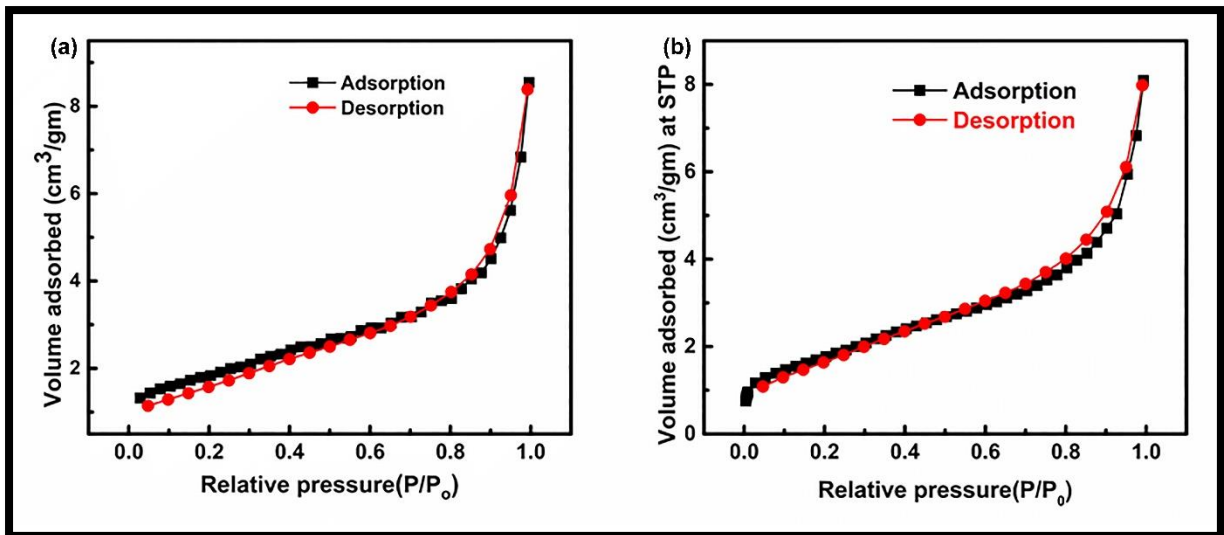


Figure S1: N_2 adsorption-desorption isotherm for (a) ONMS, and (b) NMS

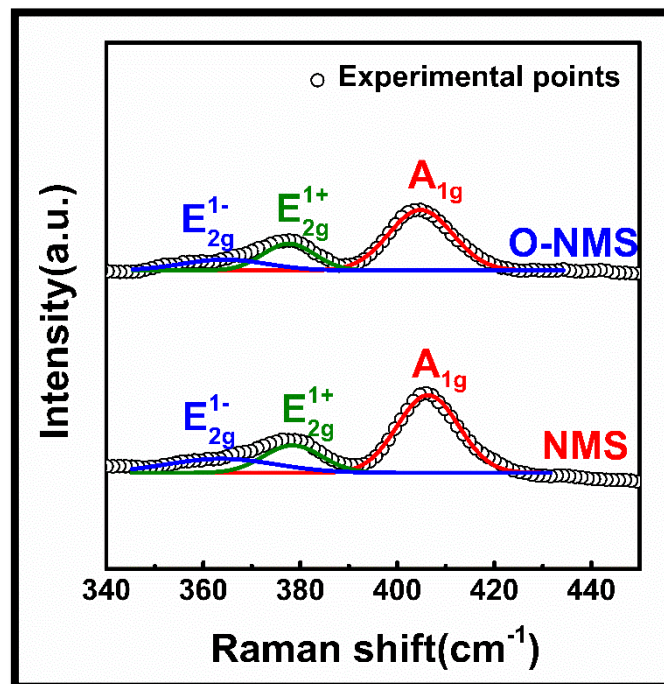


Figure S2: The E_{2g} peak splits into E_{2g}^{1+} and E_{2g}^{1-} peaks consequent to the lattice strain produced because of doping.

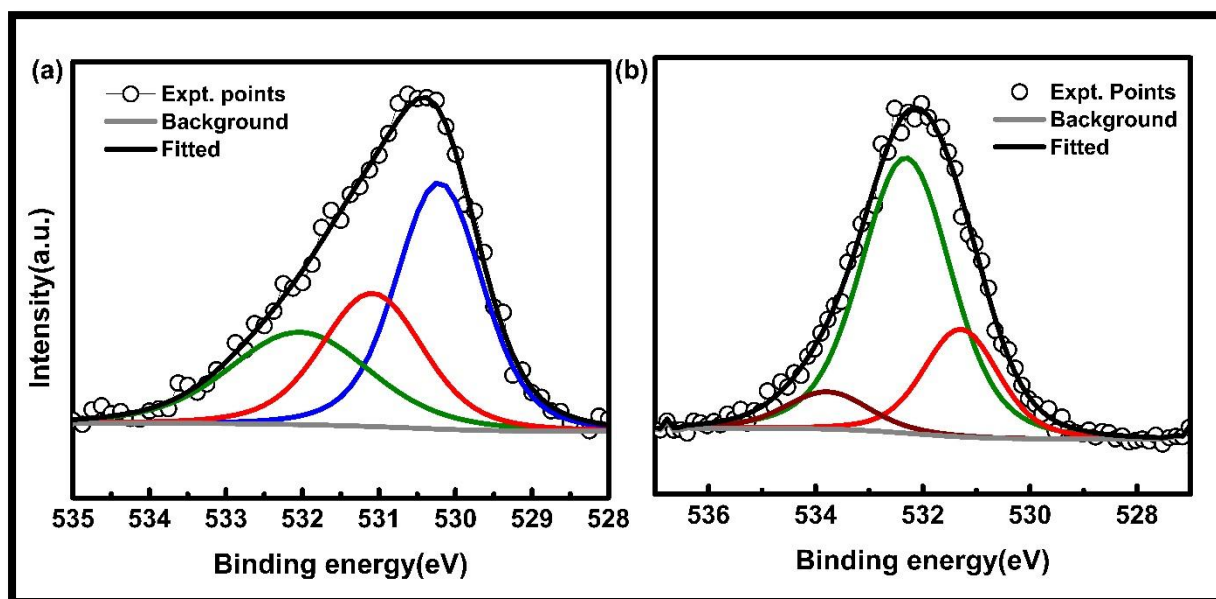
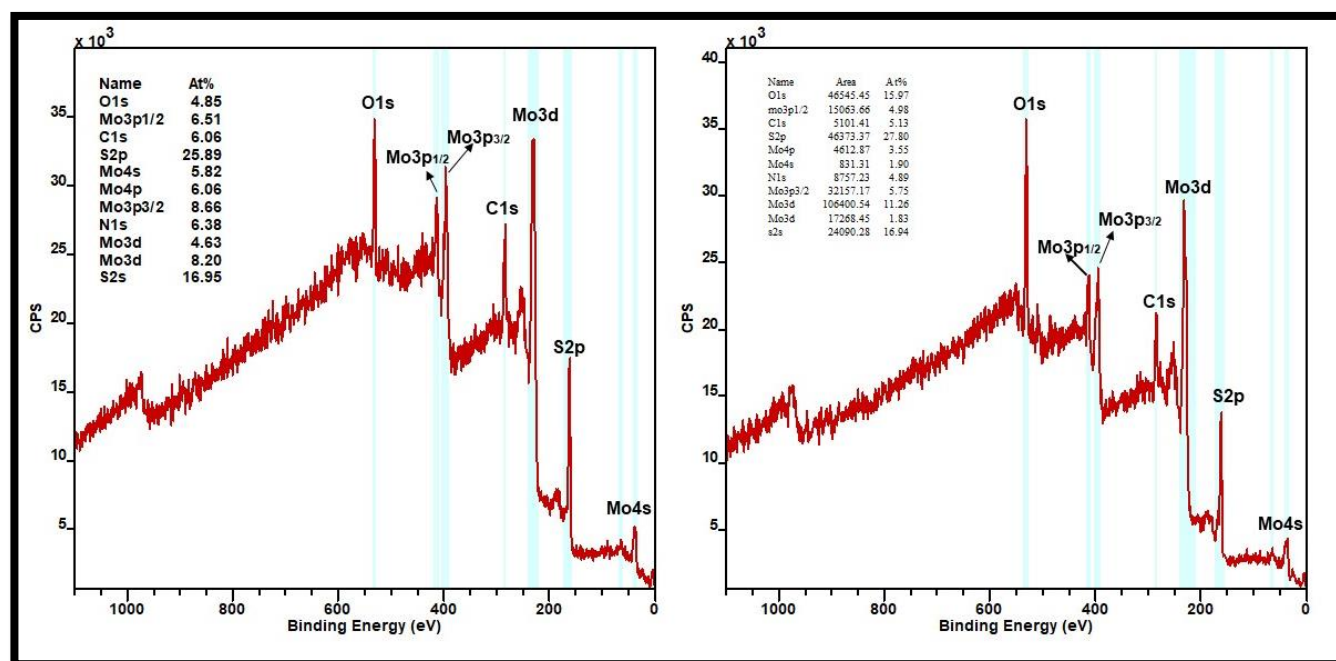


Figure S3: High resolution X-ray photoelectron spectrum from O 1s of (a) ONMS,



(b) NMS

Figure S4: XPS survey spectrum analysis of NMS and ONMS

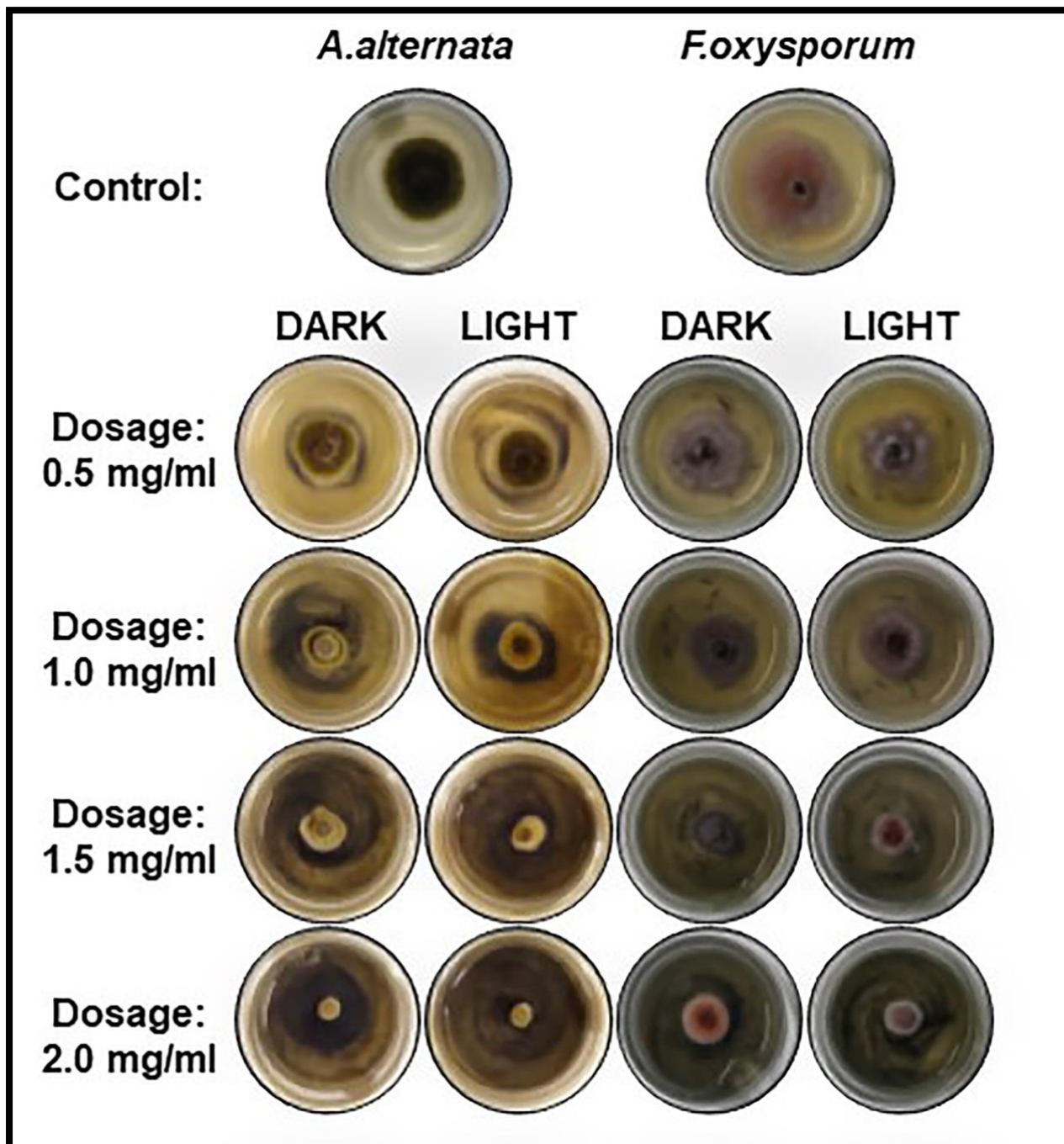


Figure S5: Digital photographs of *A.alternata* and *F.oxysporum* colonies treated with different doses of ONMS, grown in presence and absence of visible light irradiation.

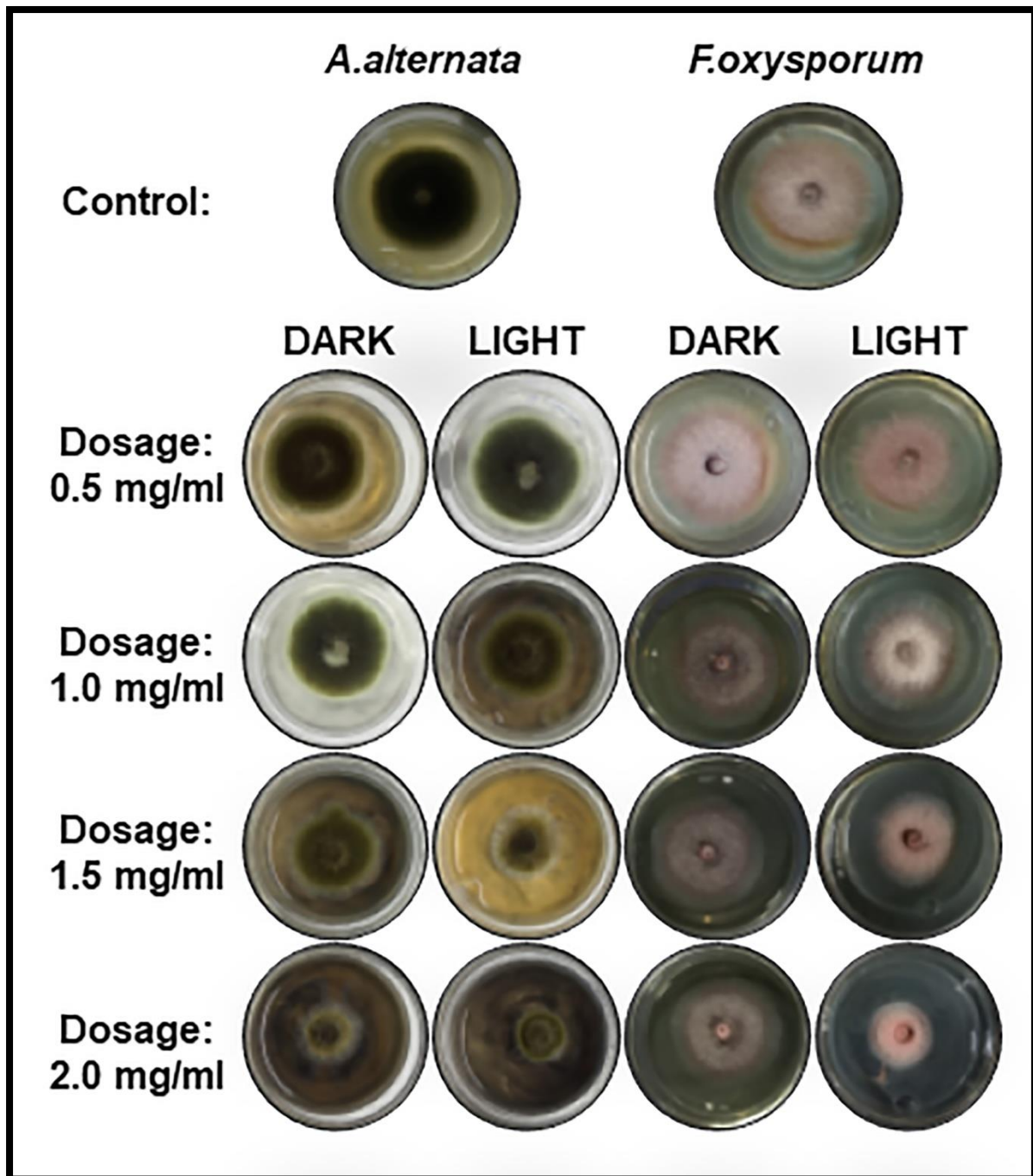


Figure S6: Dose dependent fungitoxicity of NMS towards *A.alternata* and *F.oxysporum* colonies grown in presence of and in absence of visible light irradiation.

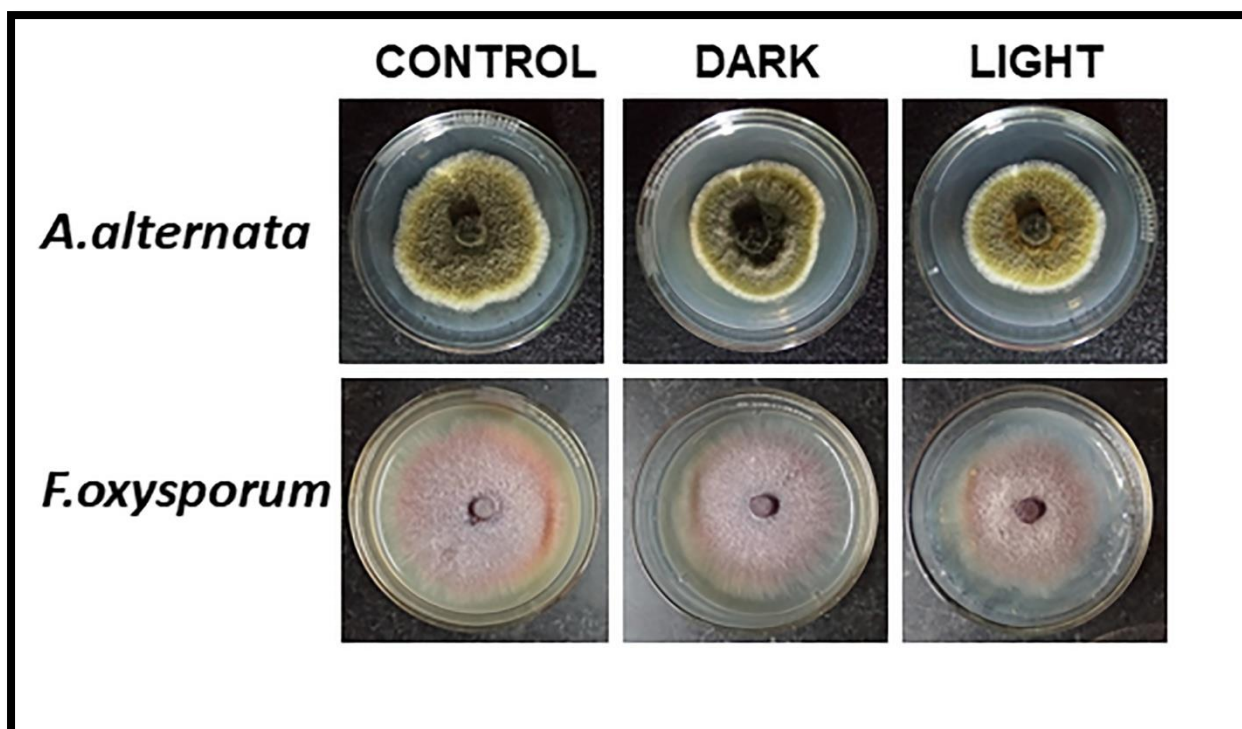


Figure S7: Non-toxicity of bare MS towards *A.alternata* and *F.oxysporum* showing no significant growth inhibition at 2 mg/ml concentration in presence/absence of visible light.

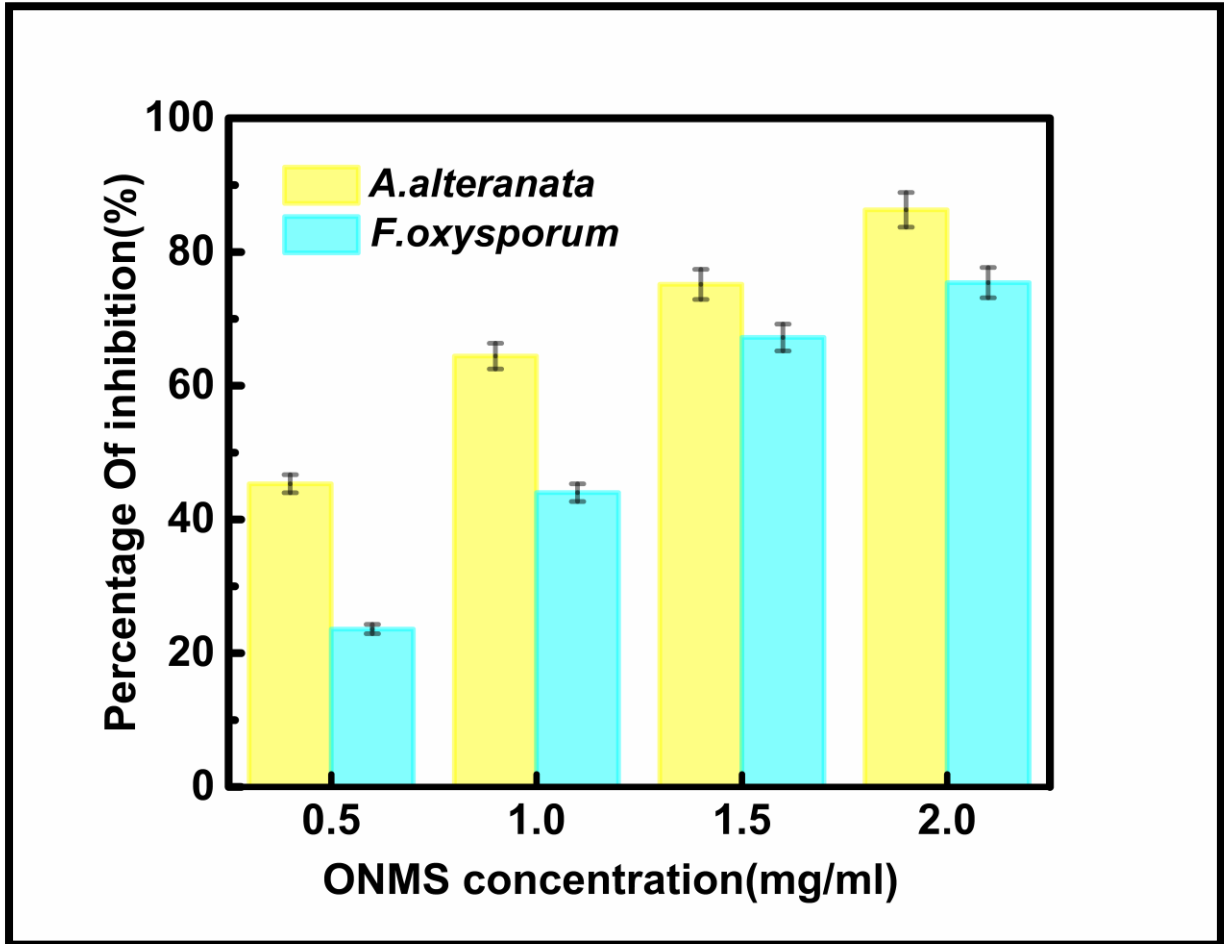


Figure S8: Dose dependent fungitoxicity assessment of ONMS towards *A.alternata* and *F.oxysporum* in liquid medium by TTC assay

Table S1: Summary of best quality 2D layered nanomaterial based reported fungicides

Nanomaterial	Morphology	Target pathogen	Whether ROS is generated, and generated in Dark/Light	Mechanism of fungitoxicity	Reference
rGO	Nanosheets	<i>Aspergillus niger</i> , <i>Aspergillus oryzae</i> , <i>Fusarium oxysporum</i>	Not mentioned	Direct contact with the sharp edges.	Sawangphruk <i>et al.</i> ²
GO	Sheets	<i>Phanerochaete hysosporium</i>	Not mentioned	No clear idea is given	Xie <i>et al.</i> ³
GO	Flat sheets	<i>Fusarium graminearum</i> , <i>Fusarium oxysporum</i>	Not mentioned	Local damaging of the cell membrane integrity subsequently causing electrolyte leakage.	Chen <i>et al.</i> ⁴
MoS ₂ loaded with Ag and Chitosan	Nanosheets	<i>Saccharomyces uvarum</i> , <i>Aspergillus niger</i>	Not mentioned	Direct cell membrane and cell wall damaging.	Zhang <i>et al.</i> ⁵
MoS ₂	Nanosheets	<i>Aspergillus niger</i> , <i>Candida sp.</i>	Not mentioned	In light(30 min) by the presence of metallic states at the edges	Karwowska <i>et al.</i> ⁶
Ag-GO	Nanosheets	<i>Fusarium graminearum</i>	ROS generated, not mentioned	Physical injury and chemical ROS generation	Chen <i>et al.</i> ⁷
O,N doped MoS ₂	Nanoflowers	<i>A.alternata</i> , <i>Fusarium oxysporum</i>	ROS generated, Both in dark and light	Transfer of elastic energy on relaxation caused ROS generation in dark which was augmented with exposure to light.	This study

S1.3 Biocompatibility assay for ONMS:

S1.3.1 Experimental:

1. Two fresh potato tubers were washed thoroughly with tap water and dipped into 0.5% Sodiumhypochlorite solution (NaOCl) for 2 mins followed by distilled water wash.

2. Both the tubers were then partially cleaved with a sharp sterilized knife.
3. One tuber was dipped into ONMS solution (2mg/ml) while the other was incubated into distilled water for 5 mins.
4. Both the tubers were taken out at the same time and incubated separately at humid chamber maintaining ~90% humidity and 30°C temperature for 7 days.

S1.3.2 Results:

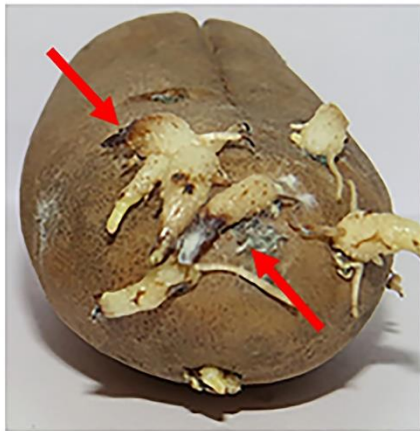
The tuber dipped into the MoS₂ nanomaterial solution appears fresh and develops no fungal growth, whereas, characteristic blackening of the surface is noticed along with some fungal growth in the untreated tuber.

S1.3.3 Discussion:

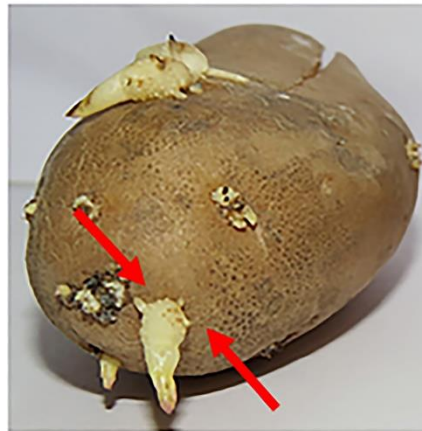
The antifungal property of the ONMS nanomaterial has successfully arrested the fungal infection in the treated tuber, while the untreated one has developed the fungal growth. Onset of pathogen in cell results in higher respiration and depletion of stored starchy materials in the potato tuber. Rapid utilization of starch accelerates dehydration of the cell and develops the characteristic blackening of the potato skin.⁸

DORSAL VIEW

Untreated

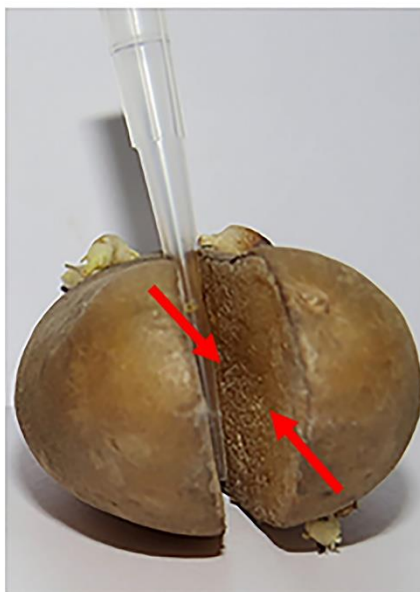


Treated



FRONT VIEW

Untreated



Treated



Figure S9: Biocompatibility assay of ONMS on potato tuber. Fungal growth on outer surface and blackening of the inner layer is indicated with red arrow.

References:

- (1) Olsen, J. V.; Kirkegaard, P.; Pedersen, N. J.; Eldrup, M. PALSfit: a new program for the evaluation of positron lifetime spectra. *Physica status solidi C* **2007**, *4* (10), 4004-4006.
- (2) Sawangphruk, M.; Srimuk, P.; Chiochan, P.; Sangsri, T.; Siwayaprahm, P. Synthesis and antifungal activity of reduced graphene oxide nanosheets. *Carbon* **2012**, *50* (14), 5156-5161.
- (3) Xie, J.; Ming, Z.; Li, H.; Yang, H.; Yu, B.; Wu, R.; Liu, X.; Bai, Y.; Yang, S.-T. Toxicity of graphene oxide to white rot fungus *Phanerochaete chrysosporium*. *Chemosphere* **2016**, *151*, 324-331.
- (4) Chen, J.; Peng, H.; Wang, X.; Shao, F.; Yuan, Z.; Han, H. Graphene oxide exhibits broad-spectrum antimicrobial activity against bacterial phytopathogens and fungal conidia by intertwining and membrane perturbation. *Nanoscale* **2014**, *6* (3), 1879-1889.
- (5) Zhang, W.; Mou, Z.; Wang, Y.; Chen, Y.; Yang, E.; Guo, F.; Sun, D.; Wang, W. Molybdenum disulfide nanosheets loaded with chitosan and silver nanoparticles effective antifungal activities: in vitro and in vivo. *Materials Science and Engineering: C* **2019**, *97*, 486-497.
- (6) Karwowska, E.; Kostecki, M.; Sokołowska, A.; Chodun, R.; Zdunek, K. Peculiar Role of the Metallic States on the Nano-M o S 2 Ceramic Particle Surface in Antimicrobial and Antifungal Activity. *International Journal of Applied Ceramic Technology* **2015**, *12* (4), 885-890.
- (7) Chen, J.; Sun, L.; Cheng, Y.; Lu, Z.; Shao, K.; Li, T.; Hu, C.; Han, H. Graphene oxide-silver nanocomposite: novel agricultural antifungal agent against *Fusarium graminearum* for crop disease prevention. *ACS applied materials & interfaces* **2016**, *8* (36), 24057-24070.
- (8) Boxi, S. S.; Mukherjee, K.; Paria, S. Ag doped hollow TiO₂ nanoparticles as an effective green fungicide against *Fusarium solani* and *Venturia inaequalis* phytopathogens. *Nanotechnology* **2016**, *27* (8), 085103.